

Galactic evolution of Copper in the light of NLTE computations [★]

S. Andrievsky^{1,2,†}, P. Bonifacio², E. Caffau², S. Korotin,^{1,3} M. Spite², F. Spite², L. Sbordone⁴ and A.V. Zhukova³

¹*Department of Astronomy and Astronomical Observatory, Odessa National University, Isaac Newton Institute of Chile, Odessa Branch, Shevchenko Park, 65014, Odessa, Ukraine*

²*GEPI, Observatoire de Paris, PSL Research University, CNRS, Place Jules Janssen, 92195 Meudon, France*

³*Crimean Astrophysical Observatory, Nauchny 298409, Republic of Crimea*

⁴*European Southern Observatory, Alonso de Cordova 3107, Vitacura, Santiago, Chile*

Accepted XXX. Received YYY; in original form ZZZ

ABSTRACT

We have developed a model atom for Cu with which we perform statistical equilibrium computations that allow us to compute the line formation of Cu I lines in stellar atmospheres without assuming Local Thermodynamic Equilibrium (LTE). We validate this model atom by reproducing the observed line profiles of the Sun, Procyon and eleven metal-poor stars. Our sample of stars includes both dwarfs and giants. Over a wide range of stellar parameters we obtain excellent agreement among different Cu I lines. The eleven metal-poor stars have iron abundances in the range $-4.2 \leq [\text{Fe}/\text{H}] \leq -1.4$, the weighted mean of the $[\text{Cu}/\text{Fe}]$ ratios is -0.22 dex, with a scatter of -0.15 dex. This is very different from the results from LTE analysis (the difference between NLTE and LTE abundances reaches 1 dex) and in spite of the small size of our sample it prompts for a revision of the Galactic evolution of Cu.

Key words: radiative transfer – line: formation – line: profiles – stars: atmospheres – stars: abundances – Galaxy: evolution

1 INTRODUCTION

Copper is an odd element that can be formed through several nucleosynthetic processes (Bisterzo et al. 2004), the relevant importance of the various processes is debatable. Up to now there has been a general consensus that, observationally, the $[\text{Cu}/\text{Fe}]$ ratio decreases with decreasing metallicity (e.g. Cohen 1980; Sneden et al. 1991; Mishenina et al. 2002; Simmerer et al. 2003; Bihain et al. 2004, see Bonifacio et al. 2010 for a concise summary of the observations). At very low metallicity the only lines that are strong enough to be measured on ground-based spectra are the UV Cu I resonant doublet at 3247 Å and 3273 Å. Bihain et al. (2004) and Bonifacio et al. (2010) pointed out that, when computed under the assumptions of Local Thermodynamic Equilibrium (LTE), these lines are discrepant with the optical lines. Roederer et al. (2014) could measure vacuum UV Cu II lines in two metal-poor stars, on spectra taken with the GHRS

and STIS spectrographs on the Hubble Space Telescope and found that they were strongly discrepant with the UV Cu I resonant lines. Collectively these observations prompt to consider the line formation of Cu I lines relaxing the hypothesis of Local Thermodynamic Equilibrium. Such an investigation was conducted by Shi et al. (2014), however they only considered the optical lines and not the UV resonant doublet. The model atom developed by Shi et al. (2014) was used by Yan et al. (2015) to investigate a sample of stars covering the range in metallicity -1.9 to -0.2 . In this investigation they confirmed the decrease of the $[\text{Cu}/\text{Fe}]$ ratios with decreasing metallicity, albeit with higher $[\text{Cu}/\text{Fe}]$ ratios at the lowest metallicity, with respect to the previous LTE analysis. In a subsequent investigation Yan et al. (2016) claimed that their NLTE analysis confirmed also the differences in Cu abundances between the high- α and low- α populations found by Nissen & Schuster (2011) in the metallicity range -1.5 to -0.4 .

The main purpose of our investigation is to see whether a NLTE approach is capable of reconciling the Cu abundances derived from the UV resonant doublet and the optical lines in metal-poor stars. For this purpose we developed a Cu model atom, and after a first validation on the spectra of the Sun and Procyon we applied it to a small sample of

[★] Based on observations taken at ESO, programmes 165.N-0276, 65.L-0165, 65.L-0507, 266.D-5655, 66.B-0378, 67.D-0439, 68.D-0546, 70.D-0009, 71.B-0529, 072.B-0585, 078.D-0643 and HST programme GO-14161

[†] E-mail: andrievskii@ukr.net

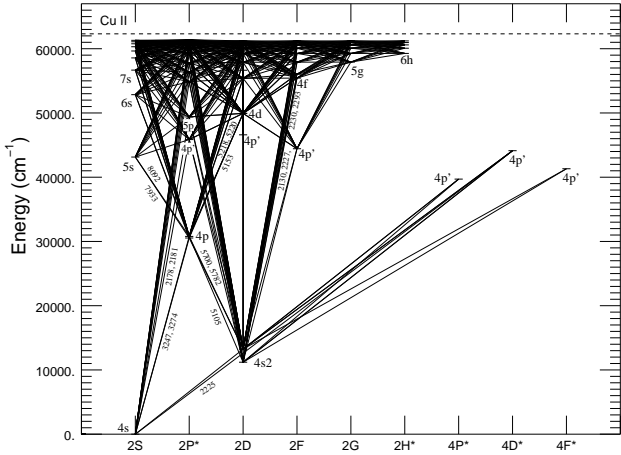


Figure 1. The Grotrian diagram of our Cu model atom.

metal-poor stars covering the range of -4.2 to -1.4 in $[\text{Fe}/\text{H}]$. When possible we complemented the ground-based spectra with vacuum UV spectra observed with Hubble Space Telescope.

2 COPPER MODEL ATOM

To build a model atom of copper we used 130 levels (116 levels of Cu I and 14 levels of Cu II). Parameters of atomic levels were taken from Liu et al. (2014), Sugar & Musgrove (1990) and the NIST database. Each LS multiplet was considered as a single term. The fine structure was taken into account for the following levels: $4s^2$ 2D, $4p^2$ P^o and $4d$ 2D, that are tightly coupled with the most important transitions in the Cu I atom (it should be noted that the fine splitting in this case is very important: for instance the splitting of $4s^2$ 2D is larger than 0.25 eV). The highest energy level in our Cu I model for which we accounted for the radiative and collisional transitions has a ionization potential 0.11 eV that corresponds to an electronic temperature of about 1300 K. Thus, we can conclude that our model describes the connection between excited levels and continuum quite accurately. The adopted Grotrian diagram of our Cu atomic model is shown in Fig. 1.

We have considered radiative transitions between the first 59 levels of Cu I and ground level of Cu II. Populations of the other levels were taken into account only in the solution of the particle number equation. All 486 bound-bound transitions were considered in detail. For each transition we accounted for Stark and van der Waals effects, as well as for the influence of the microturbulent velocity. To adequately reproduce the radiative rates of the several significant UV transitions from $4s$ 2S and $4s^2$ 2D levels we calculated the corresponding profiles for 100 to 150 frequency points. For the rest of the line profiles we used only 30 frequency points. Photoionization cross-sections were taken from Liu et al. (2014). For all the bound-bound transitions the oscillator strengths were compared to those from the NIST database, and if log gf values were absent there, we used the values provided by theoretical calculations of Liu et al. (2014).

Collisional ionization rates were calculated basing on the Seaton’s formula (Seaton 1962) with threshold photoion-

ization cross-section value from Liu et al. (2014). Collisional excitations by electrons were calculated with the help of van Regemorter’s formula (van Regemorter 1962). Collisional rates for the forbidden transitions can be found with Allen’s formula (Allen 1973) with an effective collisional strength of 1. For the 30 transitions between the low excited levels we used the collisional rates calculated by M. O’Mullane, and made available through the Atomic Data and Analysis Structure (ADAS, Summers 2004). Inelastic collisions with hydrogen atoms were described with the Drawin’s formula (Drawin 1968, 1969) adapted for astrophysical use by Steenbock & Holweger (1984).

Atomic level populations were determined using the MULTI code of Carlsson (1986) with modifications as given in Korotin et al. (1999). MULTI calculates the line profile for each line considered in detail. The line profile computed assuming either LTE or NLTE depends upon many parameters: the effective temperature of the model, the surface gravity, the microturbulent velocity, and the line damping as well as the populations in the appropriate levels. Proper comparison of observed and computed profiles in many cases requires a multielement synthesis to take into account possible blending lines of other species. For this process, we fold the NLTE (MULTI) calculations, specifically the departure coefficients, into the LTE synthetic spectrum code SYNTHV (Tsymbal 1996) that enables us to calculate the NLTE source function for copper lines. These calculations included all spectral lines from the VALD database (Ryabchikova et al. 2015) in a region of interest. The LTE approach was applied for lines other than the Cu I lines. Abundances of corresponding elements were adopted in accordance with the $[\text{Fe}/\text{H}]$ value for each star.

Cu I has several lines that are suitable for abundance determination in the visual range: 5105 Å, 5153 Å, 5218 Å, 5220 Å, 5700 Å, 5782 Å (oscillator strengths are from Kock & Richter 1968), and in IR range: 7933 Å, 8092 Å (oscillator strengths are from Carlsson 1988). Two resonance UV lines 3247 Å and 3273 Å are too strong in the solar-metallicity stars. Nevertheless, these lines can be important as a copper abundance indicator in the metal-poor stars (Bihain et al. 2004; Bonifacio et al. 2010). The log gf value for 5782 Å line is -1.78 ($\pm 12\%$) in Kock & Richter (1968), and -1.91 in Liu et al. (2014). From our solar spectrum analysis we obtained $\log gf = -1.83$. All the line parameters we used are given in Table 2. We adopted the following isotopic ratio ^{63}Cu to $^{65}\text{Cu} = 0.69/0.31$ (recommended by Grevesse et al. 2015). For most of the lines we used the hyperfine structure (*hfs*) component ratios and wavelength shifts from Shi et al. (2014). As a control, we also performed the synthesis of the Cu I line profiles in the solar spectrum using the corresponding data from Kurucz’s list (Kurucz 2014, 2011, 2005b). We did not obtain any significant differences. For the better reproduction of the profiles of the resonance doublet 3247 Å, and 3273 Å and the high excitation line 5105 Å line in the solar spectrum we used the *hfs* component shifts from the magnetic dipole splitting constants $A(J)$ and electric quadrupole splitting constants $B(J)$ from Gerstenberger et al. (1979) and Hermann et al. (1993). Components with wavelength differences less than 0.001 Å were combined into one component. Results are given in Table 2.

Since the strong Cu I lines are formed in the upper at-

Table 1. Programme stars and adopted stellar parameters.

Name	T_{eff} K	$\log g$ g in cgs	ξ km s ⁻¹	[Fe/H] dex	Ref.	A(Cu) dex
HD 111721	5095	2.64	1.4	-1.40	1	2.87 ± 0.05
HD 94028	5970	4.33	1.3	-1.47	2	2.60 ± 0.03
Cl* NGC 6752 YGN 30	4943	2.42	1.3	-1.62	3	2.35 ± 0.10
HD 9051	4925	1.95	1.8	-1.78	1	2.41 ± 0.04
HD 84937	6300	4.00	1.3	-2.25	4	1.80 ± 0.02
HD 128279	5040	2.22	1.4	-2.45	1	1.50 ± 0.06
HD 140283	5750	3.70	1.4	-2.59	5	1.40 ± 0.02
HD 122563	4600	1.10	2.0	-2.82	6	1.18 ± 0.03
CS 31082-001	4825	1.50	1.8	-2.91	6	1.35 ± 0.10
HD 200654	5007	2.21	1.0	-3.16	1	0.91 ± 0.05
CD -38° 245	4800	1.50	2.2	-4.19	6	0.04 ± 0.10

References for the atmospheric parameters

1. This paper
2. [Sitnova et al. \(2015\)](#)
3. [Yong et al. \(2008\)](#)
4. [Spite et al. \(2017\)](#)
5. [Siqueira-Mello et al. \(2015\)](#)
6. [Cayrel et al. \(2004\)](#)

atmosphere layers we applied the combination of the ATLAS solar model atmosphere of [Castelli & Kurucz \(2003\)](#) with a chromosphere from the VAL-C model [Vernazza et al. \(1981\)](#) and with corresponding distribution of the microturbulent velocity. Observed line profiles were taken from the solar flux spectrum ([Kurucz et al. 1984](#)). All the line profiles were calculated assuming the Cu meteoritic abundance ($A(\text{Cu}) = \log(\text{Cu}/\text{H}) + 12 = 4.25$, [Lodders et al. 2009](#)). To reproduce the copper lines in the solar spectrum we used the collisional rates with atomic hydrogen atoms without any correcting factor. If one uses the value adopted by [Shi et al. \(2014\)](#), then the NLTE effects lead to a significant unbalance of the calculated line intensities and this implies an increase the copper abundance in solar atmosphere. We show the calculated and observed profiles of some lines in the solar spectrum in Fig. 2. All the investigated Cu I lines are weakened by the NLTE effects. Moreover, the line cores cannot be correctly described within the LTE approximation. As a further verification of our Cu I model atom we studied the spectra of Procyon. We obtained an excellent agreement between observed and calculated Cu I profiles adopting a copper abundance $A(\text{Cu}) = 4.30 \pm 0.03$. (see Fig. 3).

3 COPPER ABUNDANCES IN STARS OF DIFFERENT METALLICITY

In order to gain some insight in the Galactic evolution of Cu we applied our model atom and NLTE analysis to a set of stars for which we could find good quality visual and UV spectra in the ESO archive and which span a large range in metallicity. We requested that for each star the spectrum of the UV doublet be available, this is covered for all stars by observations obtained with UVES. For two stars (HD 84937 and HD 140283) we could also use HST STIS spectra, that gave us access to the vacuum ultra-violet. For HD 140283 we also made use of HARPS spectra. For HD 111721, HD 9051 and HD 128279 we determined the atmospheric parameters

from the analysis of the visible spectra. We used the MyGIsFOS code ([Sbordone et al. 2014](#)) and the grids of synthetic spectra used by the MyGIsFOS code in the Gaia-ESO survey (see [Smiljanic et al. 2014](#); [Duffau et al. 2017](#)). The temperatures were derived from the iron excitation equilibrium and the surface gravities from the iron ionisation equilibrium. For the other stars we adopted atmospheric parameters from the literature. The names, adopted stellar parameters and NLTE Cu abundances are listed in Table 1.

For each star we computed a 1D LTE model atmosphere using version 9 of the ATLAS code [Kurucz \(1993, 2005a\)](#) in the Linux version detailed by [Sbordone et al. \(2004\)](#); [Sbordone \(2005\)](#) and the Opacity Distribution Functions of ([Castelli & Kurucz 2003](#)) with microturbulence of 1 km s^{-1} .

For all of the programme stars we obtain a good consistency of the abundance implied by the different lines, as shown in Fig. 4 and 5. In particular for the metal-poor giants we always obtain the consistency between the UV doublet and the high excitation 5105 \AA line. In spectra of two programme stars HD 9051 and HD 111721 the line 5218 \AA is also seen (Fig. 4). Its profile is well reproduced by our NLTE calculations. Accuracy of the profile fitting can be estimated, for instance, in Fig. 6 where we show LTE and NLTE profiles (two left panels), and NLTE profile variation with best copper abundance changed by ± 0.3 dex (two right panels). [Bonifacio et al. \(2010\)](#) pointed out that this was never possible in LTE, even when using 3D hydrodynamical simulations. In Fig. 6 and 7 we show that the NLTE profiles reproduce well the observed profiles.

We consider as a success of our NLTE model atom the fact that for HD 84937 and HD 140283 we obtain consistency between the UV doublet 3242 \AA and 3273 \AA and the vacuum UV lines: 2165 \AA , 2178 \AA , 2181 \AA , 2199 \AA , 2214 \AA , 2225 \AA , 2227 \AA , and 2230 \AA . The 3273 \AA , 2165 \AA , 2178 \AA , 2181 \AA , and 2199 \AA lines in HD 84937 and HD 140283 are shown in Fig. 8. For these two stars, we also derived the copper abundance in LTE from four Cu II lines: 2112.100 \AA , 2126.044 \AA , 2148.984 \AA and 2247.003 \AA . Our copper model atom is not designed to compute the NLTE of the Cu II transitions. Since ionised copper is the dominant species in the atmospheres of our programme stars we expect deviations from LTE to be small. The parameters of the lines were taken from the VALD database ([Ryabchikova et al. 2015](#)). We obtained $\langle(\text{Cu}/\text{H})\rangle = 1.71 \pm 0.07$ for HD 84937 and $\langle(\text{Cu}/\text{H})\rangle = 1.31 \pm 0.08$ for HD 140283. We consider the agreement satisfactory, the difference with the NLTE-results for Cu I is less than 0.10 dex. We stress that for Cu I the difference between LTE and NLTE is of 0.70–0.80 dex.

As it was noted in [Shi et al. \(2014\)](#) and [Yan et al. \(2015, 2016\)](#) the deviations from LTE lead to the copper overionization already in the deep atmosphere layers. In Fig. 9 the distribution of departure coefficients ($b_1 = \frac{n_{\text{NLTE}}}{n_{\text{LTE}}}$) are shown for Procyon (the star with solar metallicity) and the metal deficient star HD140283. As one can see, the deviations from LTE start to become important at the optical depth of about 1. For the stars with solar metallicity the resonant doublet is practically not affected by the NLTE effects. These effects are gradually increasing as metallicity decreases, and reach large values (-0.7 dex for HD 84937 and -0.75 dex for HD 140283). Subordinate copper lines show stronger NLTE

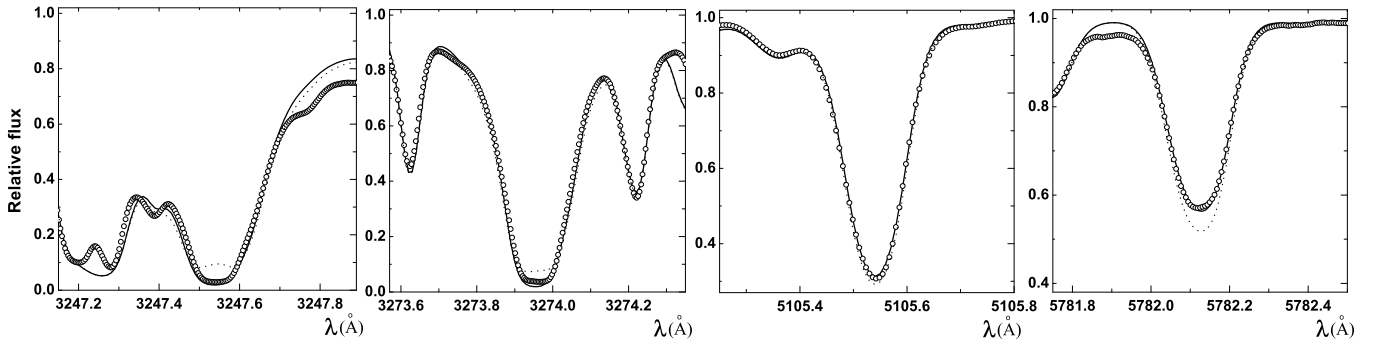


Figure 2. Several Cu I lines in the observed flux spectrum of the Sun (Kurucz et al. 1984), open circles, compared to our NLTE synthetic spectrum (solid) line and LTE synthetic spectrum (dotted line).

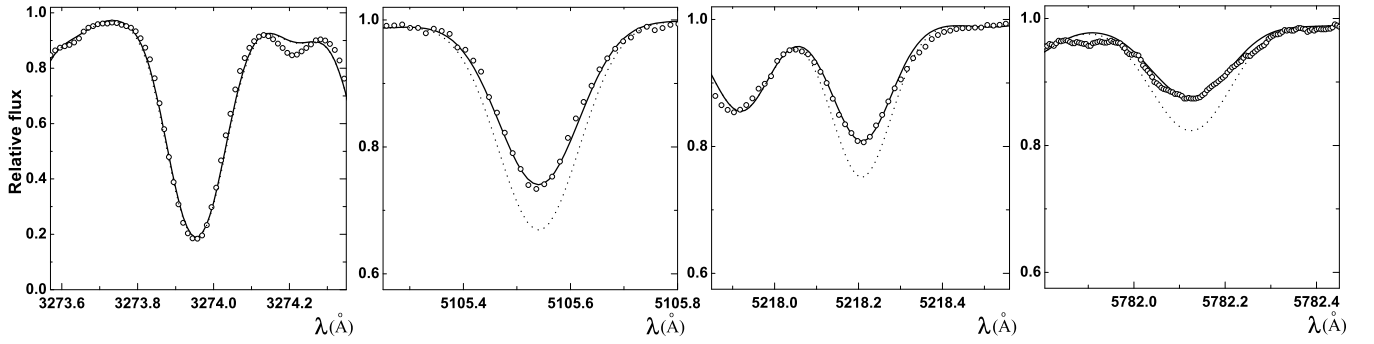


Figure 3. Several Cu I lines in the observed spectrum of the Procyon, open circles, compared to our NLTE synthetic spectrum (solid) line and LTE synthetic spectrum (dotted line).

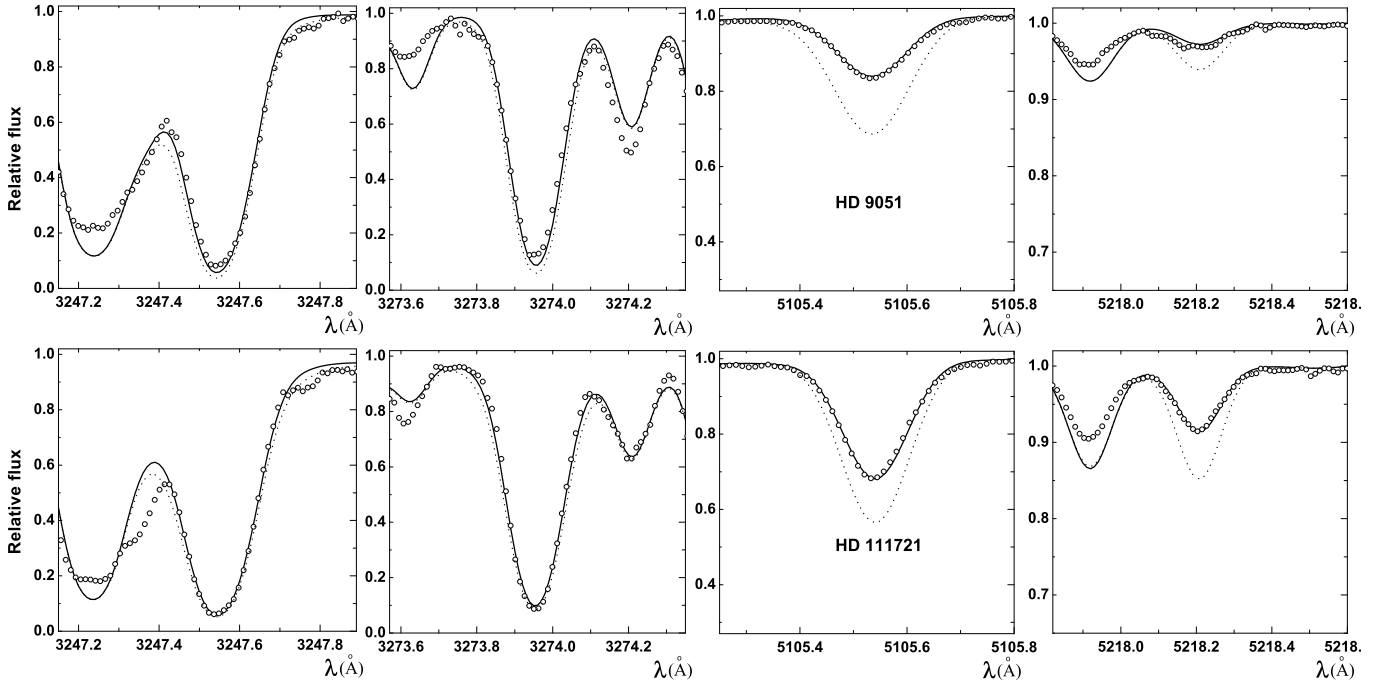


Figure 4. Cu I lines in the observed spectrum of the HD 9051 (upper panel), HD 11721 (lower panel), open circles, compared to our NLTE synthetic spectrum (solid) line and LTE synthetic spectrum (dotted line).

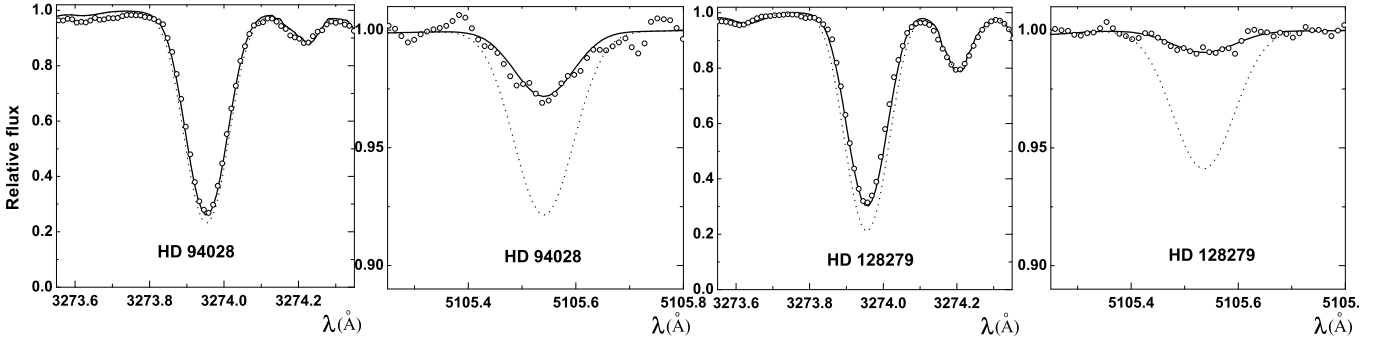


Figure 5. Cu I lines in the observed spectrum of the HD 94028 (two panels on the left) and HD 128279 (two panels on the right), open circles, compared to our NLTE synthetic spectrum (solid) line and LTE synthetic spectrum (dotted line).

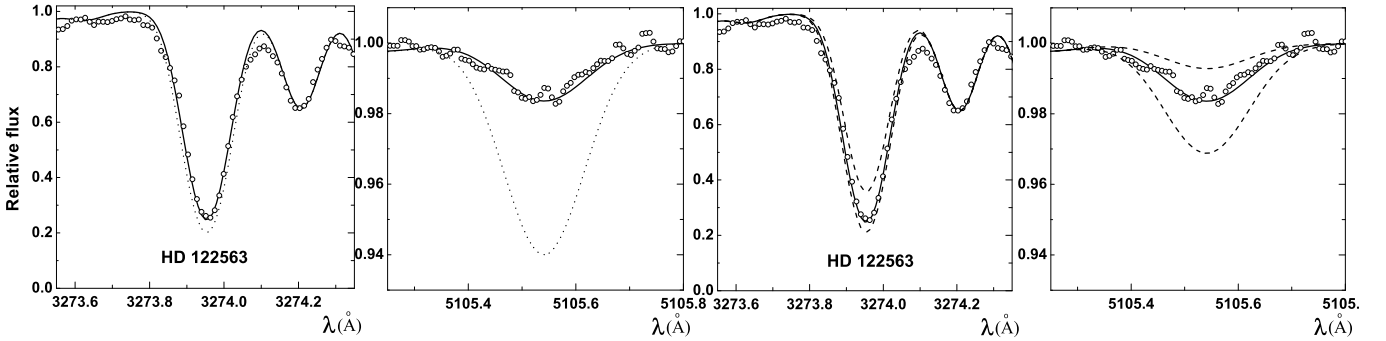


Figure 6. Cu I lines in the observed spectrum of the HD 122563, open circles, compared to our NLTE synthetic spectrum (solid) line and LTE synthetic spectrum (dotted line). The two panels on the left show the best fitting NLTE profiles, the two panels on the right show NLTE profiles computed with a Cu abundance of ± 0.3 dex of the best fitting abundance.

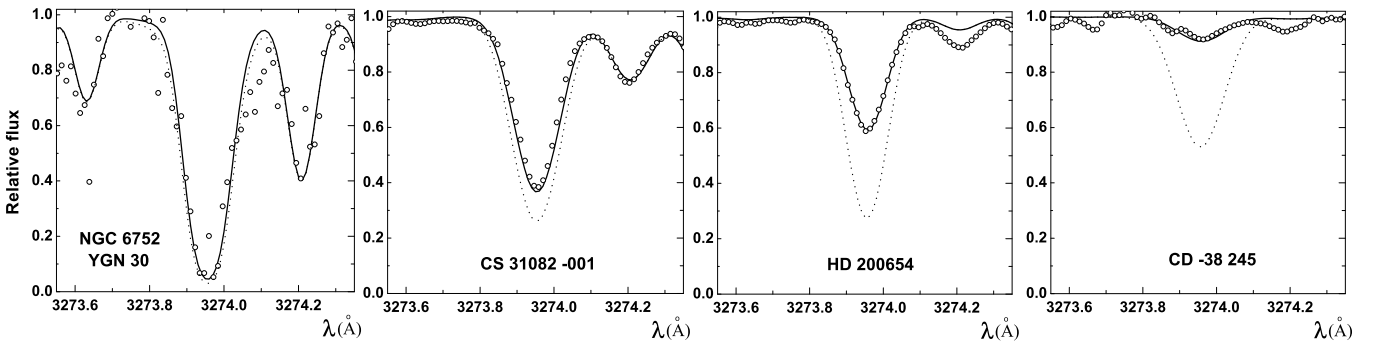


Figure 7. The Cu I 3273 Å line in Cl* NGC 6752 YGN 30, CS 31082-001, HD 200654 and CD -38°245, open circles, compared to our NLTE synthetic spectrum (solid) line and LTE synthetic spectrum (dotted line).

effects even for the stars with solar metallicity, which are seen for example in Procyon.

As in the case of UV resonance doublet, the NLTE effects increase as metallicity decreases, but with different magnitude for different lines in some cases it can be as large as 1 dex. At the same time it should be noted that in the spectra of metal-poor stars subordinate lines become too weak to be accurately measured. For the stars with T_{eff} about 6000 K and with $[\text{Fe}/\text{H}]$ of about -1.5 only the subordinate line at 5105 Å is available for analysis. In the spectra of

cooler stars, the line 5782 Å can also be seen. These lines rapidly weaken with decreasing metallicity and completely disappear in the spectra of all stars at $[\text{Fe}/\text{H}]$ of about -2.5 . The NLTE corrections significantly depend on atmospheric parameters (like T_{eff} , $\log g$, V_i , $[\text{Fe}/\text{H}]$), as well as on the copper abundance itself.

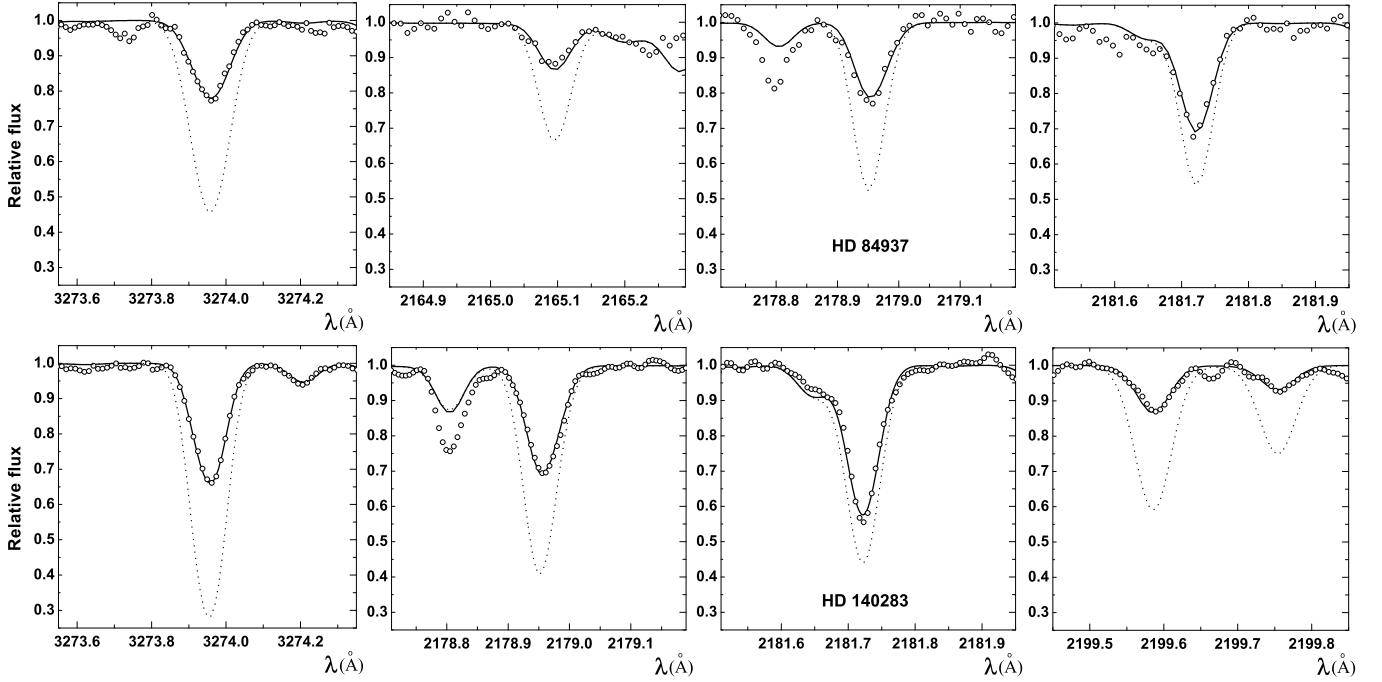


Figure 8. The Cu I 3273 Å, 2165 Å, 2178 Å, 2181 Å, and 2199 Å lines in the spectrum of the HD 84937 (upper panel) and HD 140283 (lower panel), open circles, compared to our NLTE synthetic spectrum (solid) line and LTE synthetic spectrum (dotted) line.

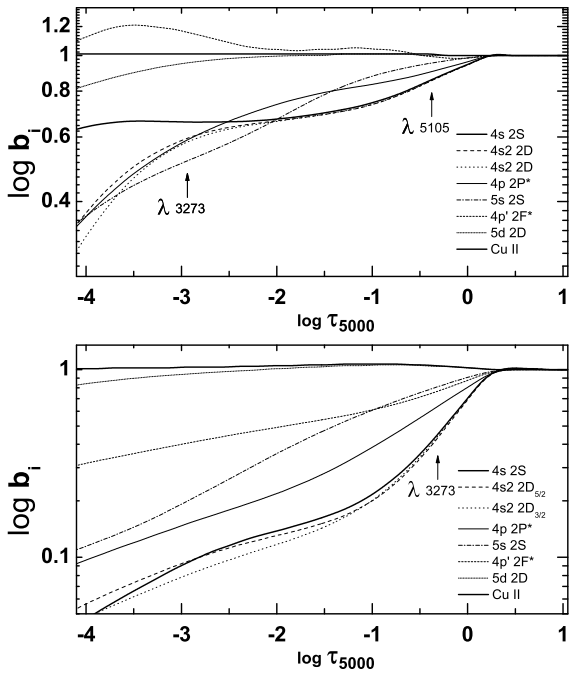


Figure 9. Computed departure coefficients as a function of optical depth in the atmosphere of Procyon (upper panel) and HD 140283 (lower panel).

4 DISCUSSION

Our sample of stars is very small and spans the metallicity range $-4.2 \leq [\text{Fe}/\text{H}] \leq -1.5$. We do not claim that we are in the best possible position to discuss the Galactic evolu-

tion of copper, yet a few results are already noticeable. The fact that our NLTE analysis derives consistent abundances from different lines, including the strong vacuum UV lines, when available, allows us to conclude that the UV resonant doublet at 3247 Å and 3273 Å is a reliable indicator of the copper abundance. This is important because this doublet is the only one available to measure the copper abundance in low metallicity stars. We consider quite remarkable that we could measure the doublet in CD-38° 245, that is, to our knowledge, the measurement of Cu at lowest metallicity so far achieved. We also checked the UVES spectra of HE 0107-5240 ($[\text{Fe}/\text{H}] = -5.46$ Christlieb et al. 2004), but we could not detect any of the two lines. Based on the UVES spectra of CD-38° 245 the lines can be detected down to $[\text{Fe}/\text{H}] = -4.8$ in cool giants. Up to now the measurements of Cu at very low metallicity (Bihain et al. 2004; Lai et al. 2008; Cohen et al. 2008; Roederer et al. 2012, 2014) rely on the UV resonant lines. Our investigation shows that these measurements have to be revised to take into account the NLTE effects on these lines.

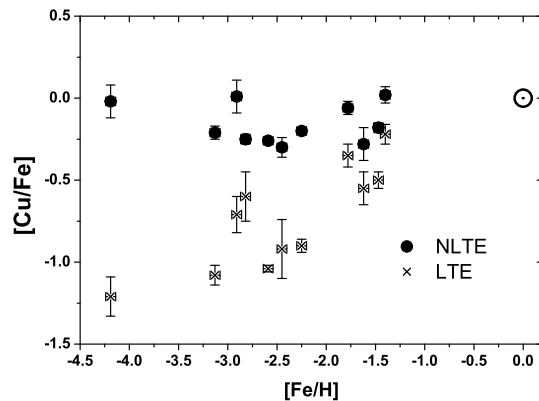
In Fig. 10 we show the run of $[\text{Cu}/\text{Fe}]$ as a function of $[\text{Fe}/\text{H}]$ for our programme stars. We also show the solar value, for reference. The main result that is apparent is that there are no very low $[\text{Cu}/\text{Fe}]$ values at variance with what happens in the LTE analysis. Our sample is more metal-poor than the sample of Yan et al. (2015), and we have only one star, HD 94028 in common. The adopted stellar parameters for this star are very close, yet we provide $[\text{Cu}/\text{Fe}] = -0.18 \pm 0.03$ while Yan et al. (2015) provide -0.32 ± 0.06 . Their abundance is based only on the 5105 Å line while ours relies also on the 2 UV resonance lines. From the 5105 Å line we derive $[\text{Cu}/\text{Fe}] = -0.14$ and from the two resonance lines -0.22 . Our NLTE correction for the 5105 Å

Table 2. Atomic data for the lines Cu I.

λ (Å)	log gf <i>hfs</i>	log gf line	Ref	λ (Å)	log gf <i>hfs</i>	log gf line	Ref
2165.096		-0.840	1	5700.143	-4.298	-2.58	3
2178.949		-0.586	1	5700.159	-4.094		
2181.722		-0.741	1	5700.164	-4.696		
2199.586		0.447	1	5700.166	-4.298		
2199.754		0.340	1	5700.173	-3.948		
2214.583		0.108	1	5700.188	-3.744		
2225.705		-1.205	1	5700.193	-4.346		
2227.776		0.460	1	5700.194	-4.152		
2230.086		0.642	1	5700.195	-3.948		
2293.844		-0.115	1	5700.200	-3.997		
				5700.205	-4.094		
3247.511	-1.379	-0.05	2	5700.221	-3.802		
3247.513	-1.028			5700.227	-3.647		
3247.515	-1.379			5700.231	-3.744		
3247.517	-0.957			5700.260	-3.550		
3247.520	-1.426			5700.266	-4.152		
3247.555	-0.288			5700.279	-3.198		
3247.558	-1.567			5700.285	-3.802		
3273.927	-1.375	-0.35	2	5782.034	-3.544	-1.83	4
3273.929	-1.024			5782.042	-3.845		
3273.931	-2.074			5782.054	-3.146		
3273.933	-1.723			5782.064	-3.196		
3273.971	-1.024			5782.073	-3.497		
3273.972	-1.375			5782.084	-2.798		
3273.975	-1.024			5782.085	-3.146		
3273.976	-1.375			5782.097	-3.146		
				5782.113	-2.798		
5105.504	-3.720	-1.51	2	5782.124	-2.798		
5105.513	-2.766			5782.153	-2.698		
5105.516	-2.813			5782.172	-2.350		
5105.517	-3.090						
5105.521	-2.720			7933.125	-0.420		5
5105.526	-2.398						
5105.536	-2.051			8092.603	-2.179	-0.16	5
5105.563	-1.942			8092.604	-1.831		
				8092.612	-0.971		
5153.232	-0.441	-0.01	2	8092.625	-0.523		
5153.241	-0.219			8092.638	-1.530		
				8092.639	-1.878		
5218.200	-0.934	0.27	2	8092.642	-1.132		
5218.202	-0.457			8092.644	-1.480		
5218.206	-0.236			8092.651	-1.132		
5218.211	-0.089			8092.653	-1.480		
5220.071	-1.816	-0.61	2				
5220.073	-1.338						
5220.077	-1.117						
5220.082	-1.131						
5220.083	-1.481						

Notes: References for log gf

1. VALD database [Ryabchikova et al. \(2015\)](#)
2. [Kock & Richter \(1968\)](#)
3. [Kurucz \(2014\)](#)
4. SUN
5. [Carlsson \(1988\)](#)


Figure 10. The Galactic evolution of Cu, as captured by our programme stars. Filled symbols are the NLTE results, \times signs are the LTE results.

line is +0.48 dex, while [Yan et al. \(2016\)](#) have a correction that is only +0.17 dex. This is certainly due to the differences between the model atoms used in the two investigations.

The lowest value of $[\text{Cu}/\text{Fe}]$ in our sample is -0.35 for HD 140283, while for the most metal-poor star in our sample, CD $-38^\circ 245$, the Cu to Fe ratio is essentially solar, like in CS 31082-001. From our sample we are not in a position to conclude in a robust way if there is a trend of $[\text{Cu}/\text{Fe}]$ with $[\text{Fe}/\text{H}]$ or if there is simply a scatter in $[\text{Cu}/\text{Fe}]$ abundances.

If we take our $[\text{Cu}/\text{Fe}]$ ratios at face value and take the mean of the sample we find $\langle [\text{Cu}/\text{Fe}] \rangle = -0.15$ with a standard deviation of 0.15 dex. The weighted mean is -0.22 dex and the mean error of unit weight ([Agekan 1972](#)) is 0.038 dex. The fact that this is smaller than the standard deviation suggests that the value of $[\text{Cu}/\text{Fe}]$ is not constant, yet the small size of our sample does not warrant any more detailed statistical analysis. We plan, in the future to apply the NLTE analysis to a much larger sample of stars for which the Cu resonance lines can be measured. A larger sample may allow to determine in a robust way the Galactic evolution of Cu.

5 CONCLUSIONS

Our NLTE model atom allows to derive consistent copper abundances from several atomic lines, over a wide range of stellar parameters, including metallicity. In agreement with previous investigations we confirm that the deviations from NLTE are larger for lower metallicities, yet our NLTE corrections are larger than those that have been found by other groups for the lines in common [Shi et al. \(2014\)](#); [Yan et al. \(2015, 2016\)](#). We have been able to show that the UV Cu I resonance lines, that are measurable down to very low metallicities ($[\text{Cu}/\text{H}] \leq -4.2$), can be used as abundance indicators, if treated in NLTE.

The influence of granulation effects on the formation of these lines remains an open issue. [Bonifacio et al. \(2010\)](#) have shown that LTE computations, based on 3D hydrodynamical simulations imply large corrections. Yet those computations were unable to achieve consistency between the UV Cu I resonant doublet and the 5105 Å line. Therefore

the issue has to be addressed by performing 3D-NLTE computations, that are not currently available.

The picture of the Galactic evolution of Cu that emerges from our analysis (see Fig. 10) is very different from what has become familiar from previous LTE analysis (Mishenina et al. 2002; Simmerer et al. 2003; Bihain et al. 2004), and that is essentially confirmed by our own LTE analysis, in spite of the limited size of the sample. Our results provide a picture that differs also from the NLTE analysis of Yan et al. (2015). Our small sample is consistent with a mean constant value of $[\text{Cu}/\text{Fe}] = -0.22$ and a scatter of 0.15 dex, in excess of the observational error for the $[\text{Fe}/\text{H}]$ range covered by our sample. A decrease of $[\text{Cu}/\text{Fe}]$ from a nearly solar value at $[\text{Fe}/\text{H}] = -1.5$ down to -0.35 at $[\text{Fe}/\text{H}] = -2.5$, followed by a steep increase to 0.0 cannot be excluded either. A much larger sample is needed to clarify the situation, it is however clear that a NLTE treatment, using our model atom, will result in $[\text{Cu}/\text{Fe}]$ ratios that are considerably larger than those found by other investigations. We can say that, by and large, Cu tracks closely Fe. This is something that models of Galactic evolution will have to take into account.

ACKNOWLEDGEMENTS

We are grateful to Ruth Peterson for giving us the reduced HST spectra that have been used in this paper and for useful comments on the manuscript. SMA is thankful to the GEPI Department and Paris Observatoire administration for their hospitality during his visit, and to the Scientific Council of Observatoire de Paris for the financial support. SAK and SMA acknowledge the partial financial support from the SCOPES grant No. IZ73Z0-152485. SAK and AVZh are thankful to the Crimean Council of Ministers for the RFBR grant No. 17-42-92008.

REFERENCES

- Agekan T. A., 1972, *Osnovi teorii osibok dla astronomov i fizikov*. Izdatel'stvo "Nauka" glavna redakcia fizicko-matematicheskog literaturi, Moskva
- Allen C. W., 1973, *Astrophysical quantities*. University of London, Athlone Press
- Bihain G., Israelian G., Rebolo R., Bonifacio P., Molaro P., 2004, *A&A*, **423**, 777
- Bisterzo S., Gallino R., Pignatari M., Pompeia L., Cunha K., Smith V., 2004, *Mem. Soc. Astron. Italiana*, **75**, 741
- Bonifacio P., Caffau E., Ludwig H.-G., 2010, *A&A*, **524**, A96
- Carlsson M., 1986, *Uppsala Astronomical Observatory Reports*, **33**
- Carlsson J., 1988, *Phys. Rev. A*, **38**, 1702
- Castelli F., Kurucz R. L., 2003, in Piskunov N., Weiss W. W., Gray D. F., eds, *IAU Symposium Vol. 210, Modelling of Stellar Atmospheres*. p. A20 ([arXiv:astro-ph/0405087](https://arxiv.org/abs/astro-ph/0405087))
- Cayrel R., et al., 2004, *A&A*, **416**, 1117
- Christlieb N., Gustafsson B., Korn A. J., Barklem P. S., Beers T. C., Bessell M. S., Karlsson T., Mizuno-Wiedner M., 2004, *ApJ*, **603**, 708
- Cohen J. G., 1980, *ApJ*, **241**, 981
- Cohen J. G., Christlieb N., McWilliam A., Shectman S., Thompson I., Melendez J., Wisotzki L., Reimers D., 2008, *ApJ*, **672**, 320
- Drawin H.-W., 1968, *Zeitschrift fur Physik*, **211**, 404
- Drawin H. W., 1969, *Zeitschrift fur Physik*, **225**, 483
- Duffau S., et al., 2017, preprint, ([arXiv:1704.02981](https://arxiv.org/abs/1704.02981))
- Gerstenberger D. C., Latush E. L., Collins G. J., 1979, *Optics Communications*, **31**, 28
- Grevesse N., Scott P., Asplund M., Sauval A. J., 2015, *A&A*, **573**, A27
- Hermann G., Lasnitschka G., Schwabe C., Spengler D., 1993, *Spectrochimica Acta*, **48**, 1259
- Kock M., Richter J., 1968, *Z. Astrophys.*, **69**, 180
- Korotin S. A., Andrievsky S. M., Luck R. E., 1999, *A&A*, **351**, 168
- Kurucz R., 1993, *ATLAS9 Stellar Atmosphere Programs and 2 km/s grid*. Kurucz CD-ROM No. 13. Cambridge, Mass.: Smithsonian Astrophysical Observatory, 1993., **13**
- Kurucz R. L., 2005a, *Memorie della Societa Astronomica Italiana Supplementi*, **8**, 14
- Kurucz R. L., 2005b, *Memorie della Societa Astronomica Italiana Supplementi*, **8**, 86
- Kurucz R. L., 2011, *Canadian Journal of Physics*, **89**, 417
- Kurucz R. L., 2014, *Problems with Atomic and Molecular Data: Including All the Lines*. pp 63–73, [doi:10.1007/978-3-319-06956-2_6](https://doi.org/10.1007/978-3-319-06956-2_6)
- Kurucz R. L., Furenlid I., Brault J., Testerman L., 1984, *Solar flux atlas from 296 to 1300 nm*
- Lai D. K., Bolte M., Johnson J. A., Lucatello S., Heger A., Woosley S. E., 2008, *ApJ*, **681**, 1524
- Liu Y. P., Gao C., Zeng J. L., Yuan J. M., Shi J. R., 2014, *ApJS*, **211**, 30
- Lodders K., Palme H., Gail H.-P., 2009, *Landolt Börnstein*, **69**, 1
- Mishenina T. V., Kovtyukh V. V., Soubiran C., Travaglio C., Busso M., 2002, *A&A*, **396**, 189
- Nissen P. E., Schuster W. J., 2011, *A&A*, **530**, A15
- Roederer I. U., et al., 2012, *ApJS*, **203**, 27
- Roederer I. U., et al., 2014, *ApJ*, **791**, 32
- Ryabchikova T., Piskunov N., Kurucz R. L., Stempels H. C., Heiter U., Pakhomov Y., Barklem P. S., 2015, *Phys. Scr.*, **90**, 054005
- Sbordone L., 2005, *Memorie della Societa Astronomica Italiana Supplementi*, **8**, 61
- Sbordone L., Bonifacio P., Castelli F., Kurucz R. L., 2004, *Memorie della Societa Astronomica Italiana Supplementi*, **5**, 93
- Sbordone L., Caffau E., Bonifacio P., Duffau S., 2014, *A&A*, **564**, A109
- Seaton M. J., 1962, in Bates D. R., ed., *Atomic and Molecular Processes*. New York: Academic Press
- Shi J. R., Gehren T., Zeng J. L., Mashonkina L., Zhao G., 2014, *ApJ*, **782**, 80
- Simmerer J., Sneden C., Ivans I. I., Kraft R. P., Shetrone M. D., Smith V. V., 2003, *AJ*, **125**, 2018
- Siqueira-Mello C., Andrievsky S. M., Barbuy B., Spite M., Spite F., Korotin S. A., 2015, *A&A*, **584**, A86
- Sitnova T., et al., 2015, *ApJ*, **808**, 148
- Smiljanic R., et al., 2014, *A&A*, **570**, A122
- Sneden C., Gratton R. G., Crocker D. A., 1991, *A&A*, **246**, 354
- Spite M., Peterson R. C., Gallagher A. J., Barbuy B., Spite F., 2017, *A&A*, **600**, A26
- Steenbock W., Holweger H., 1984, *A&A*, **130**, 319
- Sugar J., Musgrove A., 1990, *Journal of Physical and Chemical Reference Data*, **19**, 527
- Summers H. P., 2004, *The ADAS User Manual*, version 2.6, <http://www.adas.ac.uk>
- Tsymbal V., 1996, in Adelman S. J., Kupka F., Weiss W. W., eds, *Astronomical Society of the Pacific Conference Series Vol. 108, M.A.S.S., Model Atmospheres and Spectrum Synthesis*. p. 198
- Vernazza J. E., Avrett E. H., Loeser R., 1981, *ApJS*, **45**, 635
- Yan H. L., Shi J. R., Zhao G., 2015, *ApJ*, **802**, 36
- Yan H. L., Shi J. R., Nissen P. E., Zhao G., 2016, *A&A*, **585**, A102

Yong D., Meléndez J., Cunha K., Karakas A. I., Norris J. E.,
Smith V. V., 2008, *ApJ*, **689**, 1020
van Regemorter H., 1962, *ApJ*, **136**, 906

This paper has been typeset from a $\text{\TeX}/\text{\LaTeX}$ file prepared by
the author.